Noname manuscript No.
(will be inserted by the editor)

Ade Irawan · Khoirul Anwar · Tad Matsumoto

Low Complexity Time Concatenated Turbo Equalization for Block Transmission without Guard Interval: Part 3 - Application to Multiuser SIMO-OFDM

Received: date / Accepted: date

Abstract This paper proposes a Multiuser Single Input Multiple Output Orthogonal Frequency Division Multiplexing (MU-SIMO-OFDM) system without Guard Inteval (GI) based on the Chained turbo equalization (CHATUE) algorithm. Turbo equalizers for several consecutive OFDM symbols exchange information about the interference to effectively suppress inter-symbol interference (ISI), inter-carrier interference (ICI), and co-antenna interference (CAI). The convergence property of the proposed technique is analyzed using the extrinsic information transfer (EXIT) chart. Doped accumulator is used to achieve the (1,1) mutual information point and to obtain better matching between the equalizer and decoder EXIT curves. Results of computer simulations reveal that the proposed scheme can achieve excellent performance without requiring high computational complexity.

Keywords OFDM · MU-SIMO · turbo equalization · guard interval (GI) · EXIT chart · inter-symbol interference (ISI) · doped accumulator

1 Introduction

A combination of multiple input multiple output (MIMO) and orthogonal frequency division multiplexing (OFDM) appears to be one of the most efficient techniques for next generation broadband wireless systems. Standards of several communication systems such as IEEE 802.11 wireless LAN, IEEE 802.16 WiMAX, and 3GPP long term evolution (LTE) have adopted MIMO-OFDM technologies as their PHY layer spesifications. By exploiting multiple antennas at both transmitter and receiver, MIMO provides spatial multiplexing gain or diversity gain without requiring additional bandwidth or transmit power, on the top of frequency diversity obtained through channel

This work was supported in part by SANYO Electric Co., Ltd and in part by The Kinki Wireless Mobile Radio Center. The authors would like to thank them for the all support.

A. Irawan
School of Information Science, Japan Advanced Institute of Science and Technology (JAIST), 1-1 Asahidai, Nomi, Ishikawa, JAPAN 923-1292
E-mail: ade.irawan@jaist.ac.jp

K. Anwar
School of Information Science, Japan Advanced Institute of Science and Technology (JAIST), 1-1 Asahidai, Nomi, Ishikawa, JAPAN 923-1292
E-mail: anwar-k@jaist.ac.jp

T. Matsumoto
School of Information Science, Japan Advanced Institute of Science and Technology (JAIST), 1-1 Asahidai, Nomi, Ishikawa, JAPAN 923-1292
E-mail: matumoto@jaist.ac.jp
and
Center for Wireless Communication, University of Oulu, FI-90014 Finland
E-mail: tadashi.matsumoto@ee.oulu.fi

coding in OFDM. It has been shown that the capacity of MIMO systems is linearly increasing with $\min\{K_T,K_R\}$, where K_T and K_R are the numbers of transmit and receive antennas, respectively, and channels are uncorrelated [15]. This linearly increasing capacity enables MIMO systems to transmit more data with the help of multiple antennas in comparison to a single antenna system with the same bandwidth. Furthermore, OFDM signalling typically use guard interval (GI)-transmission in order to provides robustness against the fading frequency selectivity [8].

There are two types of GI-transmission schemes, one is zero padding, and the other cyclic prefix (CP)-transmission. Zero-padding-transmission places no signal duration, and use it as the guard interval. With the zero-padding transmission technique, the power efficiency loss can be avoided, while the CP-transmission introduce additional signal in front of the OFDM symbol which is a copy of the last n samples and thereby the power efficiency loss is unavoidable. However, the CP-transmission converts the block-wise channel matrix structure from Toeplitz to circulant, accordingly equivalent frequency domain channel matrix becomes diagonal. Hence, the roles of CP are twofold: (1) to prevent the OFDM signal from being distorted by inter-symbol interference (ISI) due to the channel frequency selectivity, and (2) to preserve the circulant channel structure. With the property (2), computational complexity of detection schemes, in general, with OFDM-based systems such as MIMO-OFDM can be significantly reduced.

When the length of CP is longer than the duration of the channel impulse response, ISI can completely be removed. As no new information can be transmitted during the guard interval, however, CP-transmission imposes loss in bandwidth efficiency. In order to cope with this problem and enhance the spectrum efficiency, OFDM systems with insufficient or even no CP-transmission has been considered, along with several detection approaches in literatures. Ref. [12] uses CP reconstruction technique to iteratively suppressing the inter-carrier interference (ICI) while restoring the cyclicity of the received signal when the CP length is not sufficient. By employing the interference alignment idea [4], ref. [9] proposes a channel independent precoding scheme for a MIMO-OFDM system with insufficient CP or even no CP-transmission.

Another category of technique that allows for insufficient CP-transmission is the reduced complexity frequency domain (FD) turbo equalization that well exploits the circulant structure of the frequency domain channel matrix. Ref. [5] proposes MIMO-OFDM systems without CP-transmission by assuming ISI components due to the past OFDM symbol is perfectly cancelled so that the problem comes only from the future OFDM symbol, where soft decision is employed to iteratively suppress ICI and co-antenna interference (CAI) before equalization. The FD turbo equalizer for the MIMO-OFDM systems with insufficient CP-transmission proposed in [6] performs soft interference cancellation (SC) and minimum mean square error (MMSE) filtering based on [11]. While the impact of line-of-sight (LOS) and non-LOS propagation performance are well investigated in [14].

Particularly, equalization of SIMO-OFDM sytems with insufficient CP-transmission is proposed in [3], where time domain equalization is designed with its criterion for maximizing the signal-to-interference-plus-noise ratio (SINR) and frequency domain equalization is designed for minimizing the mean-square error (MSE) of each subcarrier. Ref. [17] proposes a joint channel estimation and signal processing technique for SIMO-OFDM sytems without CP-transmission. The equalization processes consist of a ISI-free transformation [17], followed by a minimum variance filter [17]. Obviously, the low-complexity FD turbo equalization technique, originally proposed for MIMO-OFDM systems with insufficient CP-transmission [6] [14], is applicable to SIMO-OFDM.

This paper is a part-3 sister paper of its parent paper [1]. The parent paper proposes time-concatenated turbo equalization technique,referred to as Chained Turbo Equalization (CHATUE)[1][2], for block broadband single carrier transmission. The technique eliminates the necessity for the CP-transmission while preserving the beneficial points of block-wise frequency domain processing. Based on the idea, this paper for the first time extends the CHATUE algorithm to SIMO-OFDM systems without CP-transmission and provides in-depth convergence property analysis using the extrinsic information transfer (EXIT) chart. In this paper, we focus on multiuser single input multiple output (MU-SIMO)-OFDM because nowadays multiuser communications attracts a lot of attention, however, it is quite easy to modify the algorithm proposed in this paper such that it can better suited to MIMO-OFDM. This paper also has its sibling paper which applies the CHATUE algorithm to single carrier frequency division multiple access (SC-FDMA)[18].

This paper propose for MU-SIMO-OFDM systems a novel frequency domain turbo equalization technique that eliminates the necessity of CP-transmission based on the reduced complexity

frequency domain CHATUE turbo equalization algorithm proposed by [2] and [1]. The interference components due to the past and future OFDM symbols, caused by eliminating the CP, are canceled by exchanging the a posteriori log likelihood ratio (LLR) through the chained structure that connects the equalizers for the past, present, and future OFDM symbols. This paper also proposes the use of rate-1 doped accumulator for better matching of the extrinsic information transfer (EXIT) curves of the equalizer and decoder. We assess performances of the proposed MU-SIMO-OFDM without CP and conventional MU-SIMO-OFDM systems with CP-transmission. Since with the proposed CHATUE algorithm CP does not have to be transmitted, and hence the time duration made available by eliminating the CP part can also be used for transmitting more information bits or more redundant bits for error protection. A series of performance simulations were conducted to verify the superiority of the proposed technique, where for fair comparison, the coding rate was adjusted while keeping the number of the information bits in one block (including the CP length in the case of CP-transmission) constant for the both proposed and the conventional CP-transmission techniques.

The system model used in this paper is presented in Section II. Section III derives the exact version of CHATUE algorithm proposed in this paper for MU-SIMO-OFDM without CP. Furthermore, Section III modifies the exact algorithm with the aim of significantly reduce the complexity. A series of simulations was conducted to evaluate performance of the proposed CHATUE MU-SIMO-OFDM technique. Result of the EXIT analysis is first presented in Section IV to evaluate the convergence property of the proposed technique. Bit error rate (BER) performance is then presented in Section V; BER performances are compared between with and without doped accumulator as well as with and without the CHATUE algorithm. Finally, Section VI concludes this paper with several concluding statements.

The following notations are adopted in this paper. Vectors are expressed with bold lowercase, matrices with bold uppercase, and scalars with standard text notation. $\bullet^H$ and $tr(\bullet)$ denote the Hermitian(tranpose-conjugate) and the trace operation of matrix $\bullet$, respectively. $\otimes$ denotes the Kronecker product operator. A variable estimation is indicated by $\hat{\bullet}$, and expectation of random variable by $\mathbf{E}[\cdot]$. An $N \times N$ identity matrix is written as $\mathbf{I}_N$, all-one $N \times M$ matrix as $\mathbf{1}_{N\times M}$, all-zero $N \times N$ matrix as $\mathbf{0}_N$, and N-point Discrete Fourier Transform (DFT) is denoted by $\mathbf{F}_N$. Further, past and future symbols relative to the current symbol are marked with $\bullet^{'}$ and $\bullet^{''}$, respectively.

2 System Model

We consider a MU-SIMO-OFDM system with K_T users, K_R receive antennas, and N subcarriers. The channel is assumed to have L propagation paths, each separated by the symbol duration T. At each transmitter, the information bits $\mathbf{b}$ are encoded into $\mathbf{b}_C$ coded bit sequence, interleaved by a random interleaver $\mathit{\Pi}$, and doped-accumulated [13] yielding the sequence $\mathbf{x}$. By applying N-point inverse DFT (IDFT), $\mathbf{x}$ is further transformed into an OFDM symbol $\{s_{t,n}\}_{n=0}^{N-1}$ where t denotes the OFDM symbol index. The transmitted block of sample sequence in the time domain then becomes

$$\mathbf{s}_t = \{s_{t,n}^p\}_{n=0}^{N-1} \in \mathbb{C}^{NK_T\times 1} \tag{1}$$

where $p = \{1, ..., K_T\}$. The block $\mathbf{s}_t$ is transmitted over frequency-selective block quasi-static Rayleigh fading channel. Let the block-wise channel matrix at time t be denoted by

$$\mathbf{H}_t = \{\mathbf{H}_t^{i,j}\} = \begin{bmatrix} \mathbf{H}_t^{1,1} & \mathbf{H}_t^{1,2} & \dots & \mathbf{H}_t^{1,K_T} \\ \mathbf{H}_t^{2,1} & \mathbf{H}_t^{2,2} & \dots & \mathbf{H}_t^{2,K_T} \\ \vdots & \vdots & \ddots & \vdots \\ \mathbf{H}_t^{K_R,1} & \mathbf{H}_t^{K_R,2} & \dots & \mathbf{H}_t^{K_R,K_T} \end{bmatrix}_t \in \mathbb{C}^{(N+L-1)K_R\times NK_T}, \tag{2}$$

$$i = \{1, 2, ..., K_R\},$$
$$j = \{1, 2, ..., K_T\},$$

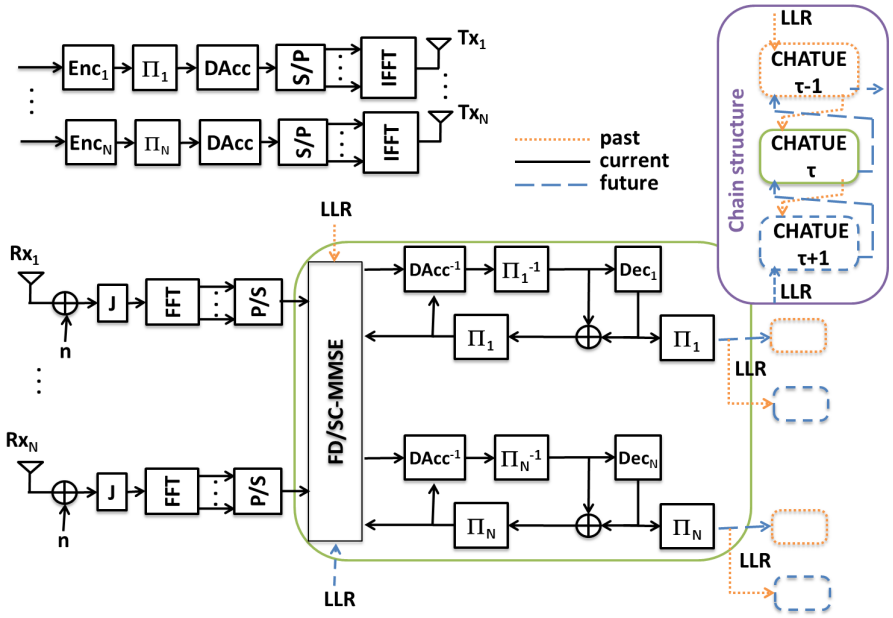

Fig. 1 MU-SIMO-OFDM Systems

where the $(N+L-1)\times N$ sub-matrix $\mathbf{H}_t^{i,j}$ has a Toeplitz structure, as

$$\mathbf{H}_t^{i,j} = \begin{bmatrix} h_0 & & 0 \\ \vdots & h_0 & \\ h_{L-1} & \vdots & \ddots \\ & h_{L-1} & \vdots \quad h_0 \\ & & \ddots \quad \vdots \\ 0 & & h_{L-1} \end{bmatrix}_t \in \mathbb{C}^{(N+L-1)\times N}, \tag{3}$$
$$i = \{1, 2, ..., K_R\},$$
$$j = \{1, 2, ..., K_T\},$$

We exploit a matrix $\mathbf{J} = \mathbf{I}_{K_R} \otimes \mathbf{J}_M$, where

$$\mathbf{J}_M = \left[\begin{array}{c|c} 0_{(N-L+1)\times(L-1)} & \mathbf{I}_N \\ \mathbf{I}_{(L-1)} & \end{array}\right] \in \mathbb{C}^{N\times(N+L-1)}, \tag{4}$$

which was introduced in [16], to convert the Toeplitz structure of the channel matrix into a circulant structure. The received composite signal can then be expressed as

$$\mathbf{r}_t = \mathbf{J}\mathbf{H}'_{t-1}\mathbf{s}'_{t-1} + \mathbf{J}\mathbf{H}_t\mathbf{s}_t + \mathbf{J}\mathbf{H}''_{t+1}\mathbf{s}''_{t+1} + \mathbf{J}\mathbf{n} \in \mathbb{C}^{NK_R\times 1}, \tag{5}$$

where $\mathbf{n}$ represents zero mean complex additive white Gaussian noise (AWGN) $K_R(N+L-1)\times 1$ matrix. The sub-matrices of the channel matrices $\mathbf{H}'_{t-1}$ and $\mathbf{H}''_{t+1}$ represent interference from the past and the future symbols, respectively, both of which have the same matrix structure as equation (2)

as $\mathbf{H}'_{t-1} = \{\mathbf{H}'^{i,j}_{t-1}\}$ and $\mathbf{H}''_{t+1} = \{\mathbf{H}''^{i,j}_{t+1}\}$, are given by

$$\mathbf{H}'^{i,j}_{t-1} = \begin{bmatrix} h_{L-1} & \cdots & h_1 \\ & \ddots & \vdots \\ & & h_{L-1} \\ 0 & & \end{bmatrix}_{t-1} \in \mathbb{C}^{(N+L-1)\times N}, \tag{6}$$

and

$$\mathbf{H}''^{i,j}_{t+1} = \begin{bmatrix} & & 0 \\ h_0 & & \\ \vdots & \ddots & \\ h_{L-2} & \cdots & h_0 \end{bmatrix}_{t+1} \in \mathbb{C}^{(N+L-1)\times N}, \tag{7}$$

respectively, and $i = \{1, 2, ..., K_R\}, j = \{1, 2, ..., K_T\}$. The received signal can then be transformed into frequency domain by DFT as

$$\begin{aligned} \mathbf{y}_t &= \mathbf{FJH}'_{t-1}\mathbf{s}'_{t-1} + \mathbf{FJH}_t\mathbf{s}_t + \mathbf{FJH}''_{t+1}\mathbf{s}''_{t+1} + \mathbf{FJn} \\ &= \mathbf{FJH}'_{t-1}\mathbf{F}^H\mathbf{x}'_{t-1} + \mathbf{FJH}_t\mathbf{F}^H\mathbf{x}_t + \mathbf{FJH}''_{t+1}\mathbf{F}^H\mathbf{x}''_{t+1} + \mathbf{FJn} \in \mathbb{C}^{NK_R\times 1}, \end{aligned} \tag{8}$$

where $\mathbf{F}$ is given by $\mathbf{F} = \mathbf{I}_{K_R} \otimes \mathbf{F}_N \in \mathbb{C}^{NK_R\times NK_R}$.

3 Proposed CHATUE Algorithm for MU-SIMO-OFDM

3.1 CHATUE Algorithm

This section derives the CHATUE algorithm for MU-SIMO-OFDM by making some modifications of the concept presented in [1] and [2]. However, since the derivation from the original algorithm shown in the Part-1 paper [1] is quite straightforward, only the part for complexity reduction, which plays a key role to make the proposed algorithm practical, are presented, and the mathematical details of the derivation are provided in Appendix for the consistency. The major difference between the proposed MU-SIMO-OFDM technique and the CHATUE Algorithm for Single Carrier are firmly discussed in Appendix.

Equalization method consists of two steps. First, we perform soft interference cancellation by subtracting the soft replica of the received signal from all antennas, yielding

$$\begin{aligned} \tilde{\mathbf{y}}_t = &\mathbf{FJH}'_{t-1}\mathbf{F}^H(\mathbf{x}'_{t-1} - \hat{\mathbf{x}}'_{t-1}) + \mathbf{FJH}_t\mathbf{F}^H(\mathbf{x}_t - \hat{\mathbf{x}}_t) \\ &+ \mathbf{FJH}''_{t+1}\mathbf{F}^H(\mathbf{x}''_{t+1} - \hat{\mathbf{x}}''_{t+1}) + \mathbf{FJn} \in \mathbb{C}^{NK_R\times 1}. \end{aligned} \tag{9}$$

Then, linear MMSE filtering is performed to further suppress the residual interference components while restoring the transmitted signal component as shown in the Appendix.

3.2 Complexity Reduction

It is well known that the complexity of the frequency domain (FD) SC/MMSE equalization is independent of the number of the propagation paths. However, the computational complexity of the block-wise processing is still large depending on the structure of the covariance matrices of the interference components, when FD SC/MMSE is applied to the CHATUE algorithm. Several approximation techniques are applied in the following sections of the paper, depending on the structure of the interference covariance matrices in order to further reduce the complexity.

We propose a technique for reducing the complexity of the matrix inversion $\mathbf{\Sigma}^{-1}$ defined by (19) in Appendix. The matrix $\mathbf{\Sigma}$, defined by (17) also in Appendix, can be divided into three parts,

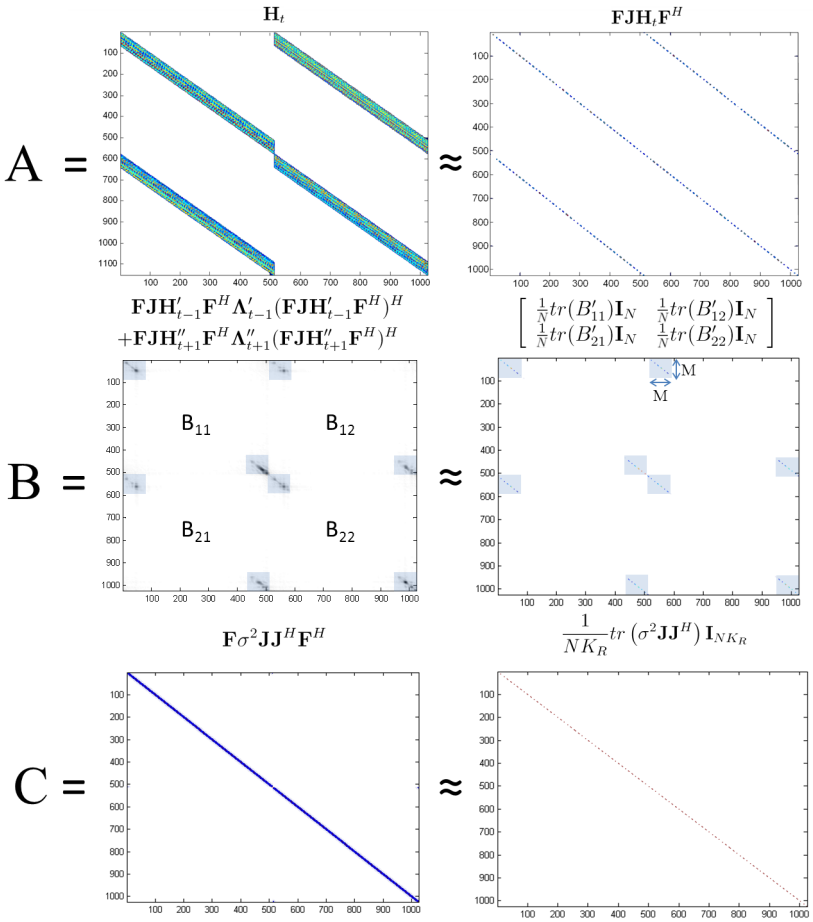

Fig. 2 Approximations of Σ at *a priori* mutual information of past and future = 0.5

matrices **A**, **B**, and **C**, where **A** stands for the covariance matrix of the residual interference in the current symbol, **B** for the covariance matrix of residual interference from the past and future components, and **C** for the noise covariance matrix. **J** matrix is utilized to convert the block-Toeplitz channel matrix $\mathbf{H}_t$ into a circulant-block matrix, which can further be converted into a diagonal block matrix in the frequency domain by exploiting DFT. Hence, as shown in Fig.2, the frequency-domain covariance matrix of the residual vector $(\mathbf{x}_t - \hat{\mathbf{x}}_t)$ in **A** can be approximated by a diagonal block matrix $\frac{1}{N}tr(\Lambda)\mathbf{I}_N$ [10].

The submatrices $\mathbf{B_{11}}$, $\mathbf{B_{12}}$, $\mathbf{B_{21}}$ and $\mathbf{B_{22}}$ in **B** contain information of the interference from the past and future symbols, and as indicated by the density in Fig. 2, each submatrix has dense part only at the top-left and bottom-right corners of the matrix. Therefore, to reduce complexity, we apply the following approximation to those *corner matrix*, as

$$\mathbf{B}_{ij} \approx \mathbf{B}'_{ij} = diag_M(\mathbf{B}_{ij}) \tag{10}$$

with $i = \{1, 2, ..., K_R\}$ and $j = \{1, 2, ..., K_T\}$ where $diag_M(\mathbf{X})$ is the operator that extracts only M diagonal elements from the top-left and bottom-right corner parts of the argument matrix **X**. Since $\mathbf{B}_{ij}$ is a diagonal elements, it is also reasonable to use the approximation :

$$\mathbf{F}_N\mathbf{B}'_{ij}\mathbf{F}_N^H = \frac{1}{N}tr(\mathbf{B}'_{ij})I_N, \tag{11}$$

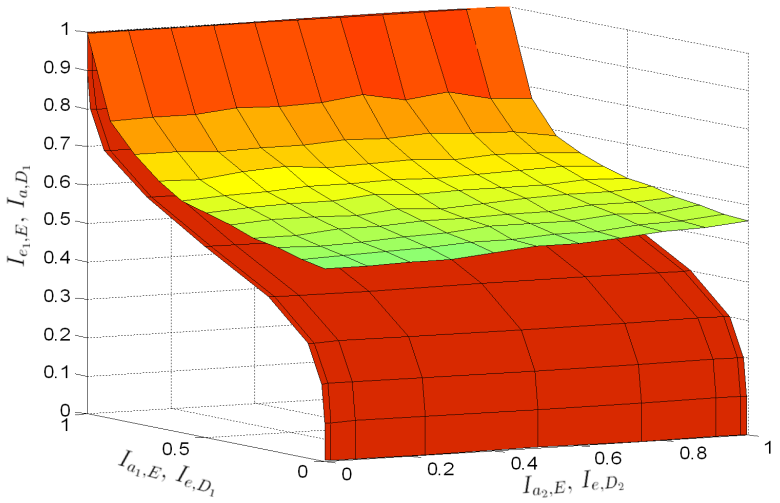

Fig. 3 Three-dimensional EXIT analysis of CHATUE-MU-SIMO-OFDM with doped accumulator at $\mathrm{E}_b/\mathrm{N}_0 = 5$ dB

with which

$$\mathbf{F}\begin{bmatrix} \mathbf{B}'_{11} & \dots & \mathbf{B}'_{1K_T} \\ \mathbf{B}'_{21} & \dots & \mathbf{B}'_{2K_T} \\ \vdots & \ddots & \vdots \\ \mathbf{B}'_{K_R1} & \dots & \mathbf{B}'_{K_RK_T} \end{bmatrix}\mathbf{F}^H = \begin{bmatrix} \frac{1}{N}tr(\mathbf{B}'_{11})I_N & \dots & \frac{1}{N}tr(\mathbf{B}'_{1K_T})I_N \\ \frac{1}{N}tr(\mathbf{B}'_{21})I_N & \dots & \frac{1}{N}tr(\mathbf{B}'_{2K_T})I_N \\ \vdots & \ddots & \vdots \\ \frac{1}{N}tr(\mathbf{B}'_{K_R1})I_N & \dots & \frac{1}{N}tr(\mathbf{B}'_{K_RK_T})I_N \end{bmatrix} \in \mathbb{C}^{NK_R \times NK_R} \tag{12}$$

Hence, it is found that as shown in Fig.2, with the approximation technique presented above, the frequency domain representation of the covariance matrix of the residual interference from the past and future symbols becomes also diagonal block matrix, given by (12).

The matrix $\mathbf{C}$ is already diagonal matrix, and hence we can use also the approximation,

$$\mathbf{F}\sigma^2\mathbf{J}\mathbf{J}^H\mathbf{F}^H \approx \frac{1}{NK_R}tr(\sigma^2\mathbf{J}\mathbf{J}^H)\mathbf{I}_{NK_R}, \tag{13}$$

as shown in the same figure. Now that we have appropriated $\mathbf{\Sigma}$ with two diagonal block and one diagonal matrices, $\mathbf{\Sigma}^{-1}$ can easily be calculated as in the original CHATUE algorithm.

4 EXIT Analysis

Result of EXIT analysis is presented in this section to evaluate the convergence property of the proposed systems. Fig. 3 shows for $\mathrm{E}_b/\mathrm{N}_0 = 5$ dB, $\mathrm{K}_T = \mathrm{K}_R = 2$, the block length $\mathrm{N} = 512$, the path number $\mathrm{L} = 64$, the approximation size $\mathrm{M} = 64$, and the doping rate $= 4$, the three-dimensional (3D) EXIT planes of the equalizer plus de-doped-accumulator (EQ+DAcc^{-1}) for the first user. *A priori* mutual information (MI) I_{a_1} and I_{a_2} are provided by the first and the second users's decoders (Dec_1^{-1} and Dec_2^{-1}, respectively) via their corresponding interleavers (Π_1 and Π_2, respectively). Equalizer's extrinsic MI of the first user is denoted by I_{e_1}. The EXIT plane for the decoder is also plotted. Note that since the both users use identical code in this case, the decoder's EXIT planes are also the same

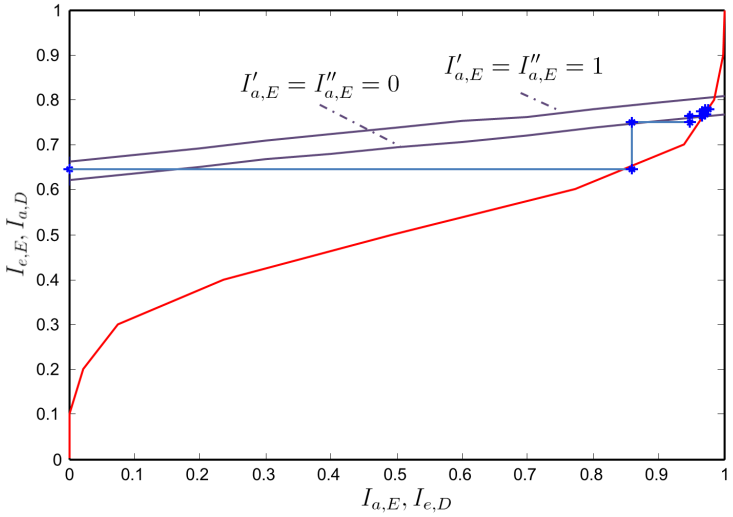

Fig. 4 EXIT analysis of CHATUE-MU-SIMO-OFDM without doped accumulator at $E_b/N_0 = 5$ dB

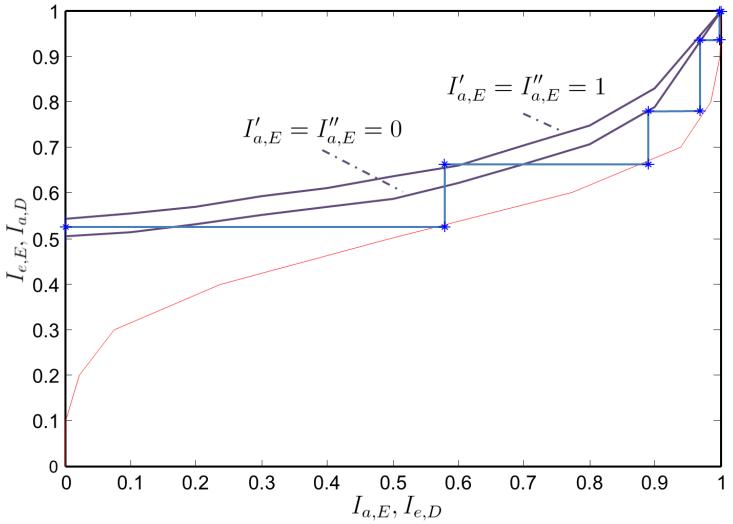

Fig. 5 EXIT analysis of CHATUE-MU-SIMO-OFDM with accumulator at $E_b/N_0 = 5$ dB

for them. For the sake of simplicity, it is assumed in this figure that the interference components from the past and the future blocks are completely cancelled. It is found from the 3D EXIT chart that the convergence tunnel opens until a point very close to the (1,1) MI point, and the larger the I_{a_2} value (*a priori* information to the equalizer fed back from the second user's decoder Dec_2^{-1}), larger the gap of the tunnel. This obviously indicates that the first user's convergence is enhanced with the help of the second user, and vice-versa.

Fig. 4 shows for the first user the EQ's projected EXIT curve and that of Dec_1^{-1}, where given the *a priori* MI I_{a_1} value, the log likelihood ratio (LLR) exchange between EQ and Dec_2^{-1} takes place as many times as until no relevant increase in the EQ's extrinsic MI I_{e_2} of the second user can be achieved, and then EQ's extrinsic MI I_{e_1} of the first user was evaluated by the on-line MI measurement method presented in [7]; this process was repeated for the other *a priori* MI values I_{a_1}, $0 \leq I_{a_1} \leq 1$.

Fig. 5 shows for the first user the projected EXIT curve of EQ+$DAcc^{-1}$ and that of Dec_1^{-1}, obtained in the same way as the projected EXIT curve shown in Fig. 4. When plotting the EXIT

Table 1 Simulation Parameters

Transmitter	Antenna	$K_T = 2, K_R = 2$
	Modulation	BPSK
	DFT/IDFT size	512
	Encoder	NSNRCC with GP = [5,7]
	Interleaver	Random
	doping ratio	1/4
Channel	Multipath Fading	64 paths, Jakes Model
Receiver	Equalizer	FD/SC-MMSE
	Iterations	10
	Channel Estimation	Perfect
	Decoder	log-MAP BCJR

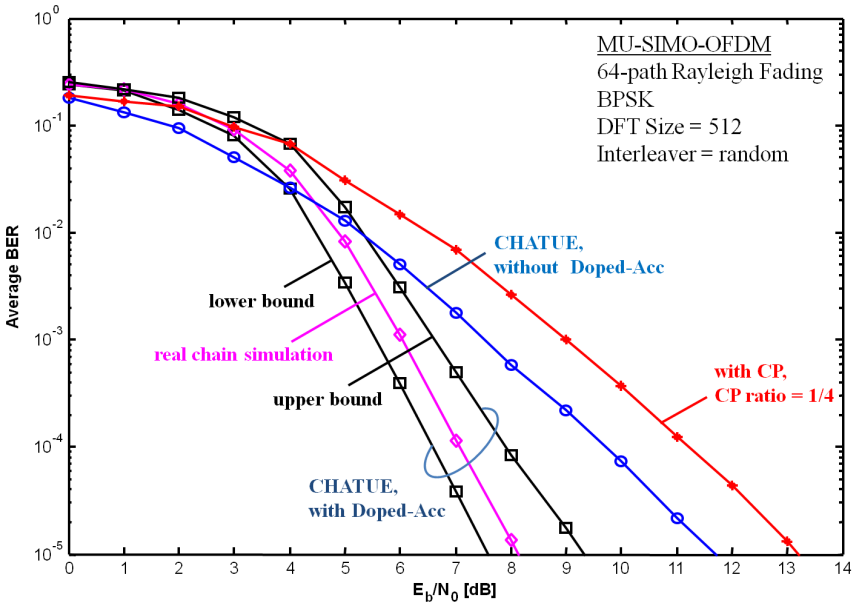

Fig. 6 BER performance of MU-SIMO-OFDM

curves in both Figs. 4 and 5, two extreme cases were assumed for the sake of simplicity. One is the case where the interference components from the past and future blocks are completely cancelled, and the other not cancelled at all, of which situations were simulated by setting the a posteriori MI provided from the decoders of the past and future blocks at 1.0 and 0.0, respectively, for the both users.

It is found from Figs. 4 and 5 that the EQ's EXIT curve increases with the help of a posteriori LLRs provided by the decoders for the past and future blocks both with and without DAcc. However, without DAcc, the EQ's projected EXIT curve does not reach a point very close to the (1,1) MI point, while with DAcc, the curve reaches the point.

In Figs. 4 and 5, trajectories obtained via chain simulation are also plotted, where initial values of MI provided by the equalizers for the past and the future blocks were set at zero, and then the MI was evaluated iteration-by-iteration accordingly, based on the LLR measurement in the chain simulation. Note that MI provided by the equalizers for the blocks of future-of-the-future and past-of-the-past are always set at zero (This setup is referred to as *truncation length* = 3 in [1]).

5 Simulation Results

We evaluated performances of conventional MU-SIMO-OFDM with a CP ratio of 1/4 with FD/SC-MMSE equalization, CHATUE-MU-SIMO-OFDM with doped accumulator, and CHATUE-MU-SIMO-OFDM without doped accumulator through computer simulations. For the CHATUE-MU-SIMO-OFDM techniques, performances were evaluated only for the reduced complexity version of the algorithm presented in Section III.B, because without the approximations, computational complexity needed to calculate the matrix inversion is excessively heavy, and thereby the beneficial points of the frequency-domain processing vanish. Simulation parameters are summarized in Table I. The channel is assumed to be equal average power block Rayleigh fading, where path coefficients are statistically independent between paths, between users, and between the receive antennas, and are constant over the block but changes block-by-block. Moreover, we assume perfect synchronism between the transmitter and receiver in terms of OFDM symbol timing, and that the receiver has perfect knowledge about the path gains of each channel, and noise variance.

Fig. 6 compares average bit error rate (BER) performance of the three MU-SIMO-OFDM techniques. Since with the proposed CHATUE algorithm, CP does not have to be transmitted, and hence the time duration made available by eliminating the CP part can also be used for transmitting more information bits or more redundant bits for error protection. For fair comparison, the coding rate was adjusted so that the number of the information bits in one block (including the CP length in the case of CP-transmission) is kept constant for the both proposed and the conventional CP-transmission techniques. For this purpose, with conventional MU-SIMO-OFDM with transmission, the bit sequence encoded by a rate 1/2 mother code was punctured so that the code rate becomes 2/3, while no puncturing was performed with the proposed CHATUE-MU-SIMO-OFDM system. Hence, the block duration, including the CP part with the conventional system, stays the same.

It can be found that without DAcc, a 2.5 dB gain in E_b/N_0 can be achieved by the CHATUE algorithm at BER = 10^{-5}, and in addition to the 2.5 dB gain, a 3.6 dB gain can be achieved by utilizing DAcc. Obviously, the 2.5 dB gain is due to the utilization of the lower rate (hence more powerful) code, made possible by eliminating the CP, and the additional 3.6 dB gain is due to the fact that the convergence tunnel opens until a point very close to the (1,1) MI point.

When evaluating the lower and upper bounds of the BER of CHATUE with DAcc, we used the same technique as that used in evaluating the trajectories. Also, we used the same technique in the chain simulation conducted to evaluate the BER performance, i.e. *truncation length* = 3, and the MI values of future-of-the-future and past-of-the-past were both set at zero. The results are shown in Fig. 6. It is found that the BER curve obtained by the real chain simulation is between the bounds.

6 Conclusion

The CHATUE algorithm has been applied to MU-SIMO-OFDM systems with the aim of eliminating the necessity for the CP-transmission. To avoid computationally heavy matrix inversion, several approximation techniques have been introduced when deriving the proposed algorithm. The ISI, ICI, and CAI components can well be suppressed by exploiting the information of interference components exchanged in the form of a posteriori LLR between the equalizers for the neighboring blocks in time. A drawback of the time-concatenation structure is the necessity of performing iterations over the neighboring equalizers. However, the computational complexity increase is only linearly in proportion to the number of the concatenated equalizer. The results of performance simulations exhibit significant improvement in E_b/N_0 required to achieve 10^{-5}, roughly 6.1 dB gain over the conventional MU-SIMO-OFDM with CP-transmission with CP ratio = 1/4. It can be concluded that the proposed systems avoids the loss in spectral efficiency due to the use of CP, while significantly improves the performances compared to the conventional MU-SIMO-OFDM systems with CP-transmission.

Appendix
Derivation of the CHATUE Algorithm

As noted in Introduction, this paper is a part-3 sister paper of the part-1 parent paper that introduces the CHATUE algorithm for single-carrier signalling, where detailed derivation of the algorithm is provided. Therefore, in Appendix of this paper, only parts which makes fundamental of difference between single carrier (part-1) and OFDM (this paper) signalling schemes are shown below.

Instead of column-wise calculation of restoral term in the soft cancellation process as introduced for the single carrier systems [1], we use block restoral term $\mathbf{\Phi}\hat{\mathbf{x}}_t$ where $\mathbf{\Phi}$ is a block diagonal matrix given by

$$\mathbf{\Phi} = \mathbf{FJH}_t\mathbf{F}^H \in \mathbb{C}^{NK_R \times NK_R} \tag{14}$$

Accordingly, the input of MMSE filter is given by

$$\begin{aligned}\bar{\mathbf{y}}_t = &\ \tilde{\mathbf{y}}_t + \mathbf{\Phi}\hat{\mathbf{x}}_t \\ = &\ \mathbf{FJH}'_{t-1}\mathbf{F}^H(\mathbf{x}'_{t-1} - \hat{\mathbf{x}}'_{t-1}) + \mathbf{FJH}_t\mathbf{F}^H(\mathbf{x}_t - \hat{\mathbf{x}}_t) \\ &+ \mathbf{FJH}''_{t+1}\mathbf{F}^H(\mathbf{x}''_{t+1} - \hat{\mathbf{x}}''_{t+1}) + \mathbf{FJn} + \mathbf{FJH}_t\mathbf{F}^H\hat{\mathbf{x}}_t \in \mathbb{C}^{NK_R \times 1}\end{aligned} \tag{15}$$

With the aid of matrix inversion lemma further weights for MMSE filtering is obtained as leads to the following expression

$$\mathbf{W}^H = \left(\mathbf{1}_{NK_T \times NK_R} + \mathit{\Gamma}\hat{\mathbf{X}}_t\right)^{-1}\mathbf{\Phi}^H\mathbf{\Sigma}^{-1} \in \mathbb{C}^{NK_R \times NK_R} \tag{16}$$

where $\hat{\mathbf{X}}_t$ is a covariance matrix of $\hat{\mathbf{x}}_t$, $\mathit{\Gamma} = \mathbf{\Phi}^H\mathbf{\Sigma}^{-1}\mathbf{\Phi}$, and $\mathbf{\Sigma}$ is given by

$$\begin{aligned}\mathbf{\Sigma} = &\ \mathbf{FJH}'_{t-1}\mathbf{F}^H\mathbf{\Lambda}'_{t-1}(\mathbf{FJH}'_{t-1}\mathbf{F}^H)^H + \mathbf{FJH}_t\mathbf{F}^H\mathbf{\Lambda}_t(\mathbf{FJH}_t\mathbf{F}^H)^H \\ &+ \mathbf{FJH}''_{t+1}\mathbf{F}^H\mathbf{\Lambda}''_{t+1}(\mathbf{FJH}''_{t+1}\mathbf{F}^H)^H + \mathbf{F}\sigma^2\mathbf{JJ}^H\mathbf{F}^H \in \mathbb{C}^{NK_R \times NK_R},\end{aligned} \tag{17}$$

with covariance matrices of the ISI components remaining in the current frame after the soft cancellation, as

$$\begin{aligned}\mathbf{\Lambda}'_{t-1} &= E\left[(\mathbf{x}'_{t-1} - \hat{\mathbf{x}}'_{t-1})(\mathbf{x}'_{t-1} - \hat{\mathbf{x}}'_{t-1})^H\right] \in \mathbb{C}^{NK_T \times NK_T}, \\ \mathbf{\Lambda}_t &= E\left[(\mathbf{x}_t - \hat{\mathbf{x}}_t)(\mathbf{x}_t - \hat{\mathbf{x}}_t)^H\right] \in \mathbb{C}^{NK_T \times NK_T}, \\ \mathbf{\Lambda}''_{t+1} &= E\left[(\mathbf{x}''_{t+1} - \hat{\mathbf{x}}''_{t+1})(\mathbf{x}''_{t+1} - \hat{\mathbf{x}}''_{t+1})^H\right] \in \mathbb{C}^{NK_T \times NK_T},\end{aligned} \tag{18}$$

and the noise variance denoted by σ^2. Finally, the equalizer output can be obtained by using (15) and (16) as

$$\begin{aligned}\mathbf{z} = \mathbf{W}^H\bar{\mathbf{y}} &= \left(\mathbf{1}_{NK_T \times NK_R} + \mathit{\Gamma}\hat{\mathbf{X}}\right)^{-1}\mathbf{\Phi}^H\mathbf{\Sigma}^{-1}(\tilde{\mathbf{y}} + \mathbf{\Phi}\hat{\mathbf{x}}) \\ &= \left(\mathbf{1}_{NK_T \times NK_R} + \mathit{\Gamma}\hat{\mathbf{X}}\right)^{-1}(\mathbf{\Phi}^H\mathbf{\Sigma}^{-1}\tilde{\mathbf{y}} + \mathit{\Gamma}\hat{\mathbf{x}}) \in \mathbb{C}^{NK_R \times 1}\end{aligned} \tag{19}$$

References

1. Anwar, K., Matsumoto, T.: Low complexity time-concatenated turbo equalization for block transmission without guard interval: Part 1 – the concept. Wireless Personal Communications (2012). DOI 10.1007/s11277-012-0563-0
2. Anwar, K., Zhou, H., Matsumoto, T.: Chained turbo equalization for block transmission without guard interval. In: IEEE VTC2010-Spring. Taiwan (2010)
3. Beheshti, M., Omidi, M., Doost-Hoseini, A.: Equalisation of simo-ofdm systems with insufficient cyclic prefix in doubly selective channels. Communications, IET **3**(12), 1870 –1882 (2009)
4. Cadambe, V.R., Jafar, S.A.: Interference alignment and the degrees of freedom for the k user interference channel. IEEE Trans. on Information Theory **54**, 3425–3441 (2008)
5. Chen, Z., Yongyu, C., Yang, D.: Low-complexity turbo equalization for MIMO-OFDM system without cyclic prefix. In: IEEE PIMRC 2009. Tokyo (2009)
6. Grossmann, M., Schneider, C., Thoma, R.: Turbo equalisation for mimo-ofdm transmission with insufficient guard interval. International Zurich Seminar on Communications **0**, 114–117 (2006). DOI http://doi.ieeecomputersociety.org/10.1109/IZS.2006.1649093
7. Hagenauer, J.: The exit chart – introduction to extrinsic information transfer in iterative processing (2004)
8. Heiskala, J., Terry, J.: OFDM Wireless LANs: A Theoretical and Practical Guide. Sams Publishing (2002)

9. Jin, Y., Xia, X.G.: A channel independent precoding for mimo-ofdm systems with insufficient cyclic prefix. In: Global Telecommunication Conference (GLOBECOM 2011), pp. 1–5. Houston, Texas, USA (2011)
10. Kansanen, K., Matsumoto, T.: An analytical method for MMSE MIMO turbo equalizer EXIT chart computation. IEEE Trans. Wireless Comm. **6**(1), 59–63 (2007)
11. Kansanen, K., Schneider, C., Matsumoto, T., Thoma, R.: Multilevel-coded qam with mimo turbo-equalization in broadband single-carrier signaling. Vehicular Technology, IEEE Transactions on **54**(3), 954 – 966 (2005)
12. Lim, J.B., Choi, C.H., Im, G.H.: MIMO-OFDM with insufficient cyclic prefix. In: IEEE Communications Letter, vol. 10, pp. 356–358 (2006)
13. Pfletschinger, S., Sanzi, F.: Error floor removal for bit-interleaved coded modulation with iterative detection. IEEE Trans. on Wireless Comm. **5**(11), 3174–3181 (2006)
14. Schneider, C., Grossmann, M., Thoma, R.: Measurement based performance evaluation of mimo-ofdm with turbo-equalization. In: Vehicular Technology Conference, 2005. VTC 2005-Spring. 2005 IEEE 61st, vol. 3, pp. 1701 – 1705 Vol. 3 (2005)
15. Telatar, E.: Capacity of multi-antenna Gaussian channels. European Trans.Telecomm **10**, 585–595 (1999)
16. Wang, D., Wei, C., Pan, Z., You, X., Kyuu, C.H., Jang, J.B.: Low-complexity turbo equalization for single-carrier systems without cyclic prefix. In: IEEE ICC, pp. 1091–1095. Beijing (2008)
17. Yu, J.L., Lee, M.C., Chen, C.H.: Finite sample performance of channel estimation and equalization for simo ofdm systems without cyclic prefix. In: TENCON 2007 - 2007 IEEE Region 10 Conference, pp. 1 –4 (2007)
18. Zhou, H., Anwar, K., Matsumoto, T.: Low complexity time-concatenated turbo equalization for block transmission without guard interval: Part 2 – application to sc-fdma. Wireless Personal Communications (2011). DOI 10.1007/s11277-011-0409-1